



OPEN

Artificial intelligence in detecting temporomandibular joint osteoarthritis on orthopantomogram

Eunhye Choi¹, Donghyun Kim², Jeong-Yun Lee³ & Hee-Kyung Park¹✉

Orthopantomogram (OPG) is important for primary diagnosis of temporomandibular joint osteoarthritis (TMJOA), because of cost and the radiation associated with computed tomograms (CT). The aims of this study were to develop an artificial intelligence (AI) model and compare its TMJOA diagnostic performance from OPGs with that of an oromaxillofacial radiology (OMFR) expert. An AI model was developed using Karas' ResNet model and trained to classify images into three categories: normal, indeterminate OA, and OA. This study included 1189 OPG images confirmed by cone-beam CT and evaluated the results by model (accuracy, precision, recall, and F1 score) and diagnostic performance (accuracy, sensitivity, and specificity). The model performance was unsatisfying when AI was developed with 3 categories. After the indeterminate OA images were reclassified as normal, OA, or omission, the AI diagnosed TMJOA in a similar manner to an expert and was in most accord with CBCT when the indeterminate OA category was omitted (accuracy: 0.78, sensitivity: 0.73, and specificity: 0.82). Our deep learning model showed a sensitivity equivalent to that of an expert, with a better balance between sensitivity and specificity, which implies that AI can play an important role in primary diagnosis of TMJOA from OPGs in most general practice clinics where OMFR experts or CT are not available.

Temporomandibular joint osteoarthritis (TMJOA) is an important subtype of temporomandibular disorders (TMDs) and may lead to substantial joint pain, dysfunction, dental malocclusion, and reduced health-related quality of life¹. Osteoarthritis (OA) is a disease of joints caused by a series of degenerative processes including gradual loss of joint cartilage, remodeling and hardening of subchondral bone, and formation of osteoproliferative bodies². TMJOA is confirmed by structural bony changes observed on radiographic examination. Because of the ability to show minute changes in the integrity of the cortical and subcortical bone of the TMJ, it is widely accepted that computed tomography (CT) is the reference standard for the diagnosis of TMJOA³. Cone beam CT (CBCT), which has the benefit of lower radiation exposure than conventional CT, is reportedly as accurate for the detection of TMJOA⁴. However, CBCT is not the first choice for TMJOA examination in the normal clinical setting yet because it still has a higher radiation dose and is costlier than plain radiographs. Normally, the orthopantomogram (OPG) is the most common examination method used for screening various lesions and conditions in the maxillofacial region, while it is less able to identify bony changes in the TMJ structure that are small in size and overlapped by other skull structures⁵. This makes OPG useful for screening examinations that experienced experts such as oromaxillofacial radiology (OMFR) or orofacial pain specialists read and then recommend, if necessary, an additional CBCT to confirm a diagnosis. In a situation where such experts are not available, a patient's TMJOA can be overlooked or misread. To address this possibility, an AI algorithm was developed and trained to read TMJOA on OPGs based on CBCT results already confirmed by experts. Various studies have applied AI algorithms to read OPG for clinical conditions such as tooth segmentation⁶, age estimation⁷, third molar and inferior alveolar nerve detection⁸, cysts and tumors of the jaw⁹, osteoporosis¹⁰, and maxillary sinusitis¹¹. However, there are few AI studies on TMJOA diagnosis; one study that used CBCT and one study based on OPG have been reported^{12,13}.

¹Department of Oral Medicine and Oral Diagnosis, School of Dentistry and Dental Research Institute, Seoul National University, #101, Daehak-ro, Jongro-gu, Seoul 03080, Korea. ²Department of Advanced General Dentistry, Yonsei University College of Dentistry, Seoul 03722, Korea. ³Seoul Cheongchoon Dental Clinic, Seoul 03086, Korea. ✉email: dentopark@snu.ac.kr

| | | Normal | Indeterminate | OA |
|--------|------------------|-------------|---------------|-------------|
| Female | Number of joints | 619 | 656 | 683 |
| | Mean age | 34.70 | 34.03 | 41.48 |
| | 95% CI | 33.56–35.83 | 32.92–35.14 | 40.23–42.73 |
| | SD | 14.43 | 14.54 | 16.66 |
| Male | Number of joints | 181 | 123 | 116 |
| | Mean age | 31.86 | 28.20 | 32.88 |
| | 95% CI | 29.78–33.94 | 26.11–30.28 | 29.88–35.88 |
| | SD | 14.27 | 11.78 | 16.50 |
| Total | Number of joints | 800 | 779 | 799 |
| | Mean age | 34.06 | 33.11 | 40.23 |
| | 95% CI | 33.06–35.05 | 32.11–34.11 | 39.06–41.40 |
| | SD | 14.43 | 14.28 | 16.89 |

Table 1. Clinical and demographic characteristics of the OPG dataset. Indeterminate, indeterminate temporomandibular joint osteoarthritis; OA, temporomandibular joint osteoarthritis.

| Confusion matrix | | | | Model performance | | | | | |
|------------------|-----------|---------------|-----|-------------------|--------|----------|----------------------------|-------------------------|----------|
| Actual | Predicted | | | Precision | Recall | Accuracy | Weighted average precision | Weighted average recall | F1 score |
| | Normal | Indeterminate | OA | | | | | | |
| Normal | 57 | 46 | 47 | 0.72 | 0.38 | 0.51 | 0.55 | 0.51 | 0.53 |
| Indeterminate | 14 | 53 | 83 | 0.44 | 0.35 | | | | |
| OA | 8 | 22 | 120 | 0.48 | 0.80 | | | | |

Table 2. Confusion matrix and model performance for the initial AI. Indeterminate, indeterminate temporomandibular joint osteoarthritis; OA, temporomandibular joint osteoarthritis.

| Confusion matrix | | | | Model performance | | | | | |
|------------------|--------|-----------|-----|-------------------|--------|----------|----------------------------|-------------------------|----------|
| | Actual | Predicted | | Precision | Recall | Accuracy | Weighted average precision | Weighted average recall | F1 score |
| | | Normal | OA | | | | | | |
| Trial 1 | Normal | 283 | 17 | 0.80 | 0.94 | 0.80 | 0.81 | 0.80 | 0.80 |
| | OA | 72 | 78 | 0.82 | 0.52 | | | | |
| Trial 2 | Normal | 35 | 115 | 0.81 | 0.23 | 0.73 | 0.75 | 0.73 | 0.74 |
| | OA | 8 | 292 | 0.72 | 0.97 | | | | |
| Trial 3 | Normal | 119 | 26 | 0.78 | 0.82 | 0.78 | 0.78 | 0.78 | 0.78 |
| | OA | 34 | 93 | 0.78 | 0.73 | | | | |

Table 3. Confusion matrix and model performance in each Trial. OA, temporomandibular joint osteoarthritis.

This study aimed to investigate the clinical utility of an AI diagnostic tool developed for TMJOA diagnosis from OPG using deep learning that compared the AI read with that of an expert.

Results

The results of the AI algorithm that was developed based on 3 categories, normal, indeterminate, and OA, are shown in Table 1. Because overall accuracy was not satisfying (Table 2), the model development process was modified and reevaluated because indeterminate TMJOA could have compromised AI training because of its vagueness on radiographic reading^{14,15}. The AI was trained, validated, and tested again in 3 ways after modification. Indeterminate OA was considered as normal in Trial 1, OA in Trial 2, and omitted from the whole development process in Trial 3. The accuracy of the model performance was best in Trial 1 (0.80) followed by Trial 3 (0.78) and Trial 2 (0.73), but precision and recall were evenest in Trial 3 (Table 3). The recall value of TMJOA was 0.51, which means that the model predicted TMJOA in patients with actual TMJOA about half the time in Trial 1. In screening tests, it is important to suspect the presence of the disease so that additional tests can be performed if necessary. For this reason, Trial 3 was chosen as a more suitable model in spite of the higher overall accuracy seen in Trial 1. Five-fold cross validation was performed on Trial 3. The average accuracy, precision, recall, and F1 score were 0.76, 0.80, 0.71, and 0.75, respectively (Table 4).

| Work | Precision | Recall | F1 score | Accuracy | AUC (95% CI) |
|---------|-----------|--------|----------|----------|------------------|
| 1 | 0.82 | 0.59 | 0.69 | 0.74 | 0.83 (0.79–0.88) |
| 2 | 0.80 | 0.71 | 0.75 | 0.77 | 0.86 (0.82–0.90) |
| 3 | 0.83 | 0.76 | 0.79 | 0.81 | 0.87 (0.83–0.91) |
| 4 | 0.75 | 0.76 | 0.75 | 0.75 | 0.83 (0.79–0.88) |
| 5 | 0.77 | 0.74 | 0.76 | 0.76 | 0.84 (0.80–0.89) |
| Average | 0.80 | 0.71 | 0.75 | 0.76 | 0.85 (0.81–0.89) |

Table 4. Five-fold cross-validation in Trial 3.

| | | Diagnostic performance | | | Cohen's kappa | Kappa index | McNemar's test |
|---------|--------|------------------------|-------------|-------------|---------------|-------------|----------------|
| | | Accuracy | Sensitivity | Specificity | | | |
| Trial 1 | Expert | 0.81 | 0.61 | 0.91 | 0.54 | Moderate | .001 |
| | AI | 0.80 | 0.52 | 0.94 | 0.51 | Moderate | .000 |
| Trial 2 | Expert | 0.69 | 0.57 | 0.93 | 0.42 | Moderate | .000 |
| | AI | 0.73 | 0.97 | 0.23 | 0.25 | Fair | .000 |
| Trial 3 | Expert | 0.85 | 0.72 | 0.97 | 0.69 | Substantial | .000 |
| | AI | 0.78 | 0.73 | 0.82 | 0.56 | Moderate | .366 |

Table 5. Diagnostic performance and level of agreement in each Trial. AI, artificial intelligence.

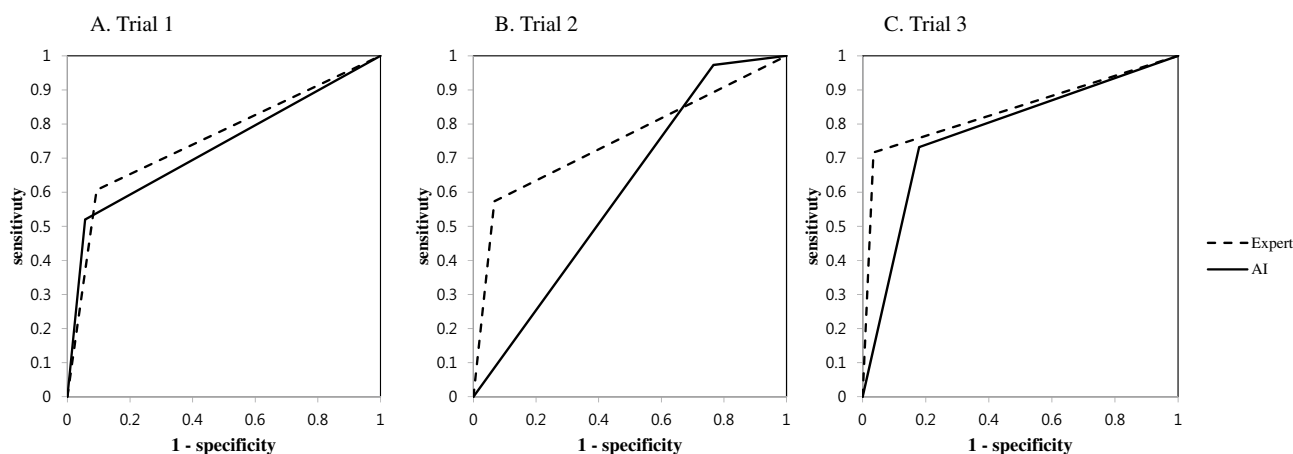


Figure 1. Comparison of the sensitivities and specificities in Trials 1, 2, and 3.

The diagnostic performance of the AI and expert and agreement between their OPG read and CBCT reads is shown in Table 5. The comparison of sensitivities and specificities in Trials 1, 2, and 3 are shown in Fig. 1. The AI in Trial 1 (0.80) and the expert in Trial 3 (0.85) were the most accurate, respectively. However, taking sensitivity and specificity into consideration collectively, it can be said that Trial 3 was the most accurate (0.85 for the expert and 0.78 for the AI). Cohen's kappa was highest as well in Trial 3 and showed a substantial level of agreement for the expert (0.69) and moderate agreement for the AI (0.56). In all 3 trials, the expert read more accurately than the AI. However, the result of McNemar's test showed that AI reads were more in accord with CBCT ($p = 0.366$) in Trial 3 where TMJOA was diagnosed dichotomously.

Discussion

OPG is the most widely used plain radiograph method for the primary diagnosis of TMJOA. However, OMFR experts or CBCT are not always available in most general practice clinics and screening for TMJOA is easily compromised. As reported previously, age, pain, and TMJ noise were not correlated with TMJOA on CBCT, while a high incidence rate for OA changes in TMD patients was observed (27.3%)¹⁶. It was also reported that 24% of patients who did not show significant condyle bone changes on OPG had degenerative bone changes on CBCT¹⁷. Moreover, it is also very well known that the accuracy, sensitivity, and specificity of OPG is not good for the diagnosis of TMJOA, even when an expert OMFR radiologist reads OPG images. OPG showed lower sensitivity (0.26) and higher specificity (0.99) compared to CT in TMJOA patients¹⁴. The diagnostic accuracy of OPG

for detecting cortical erosion of the mandibular condyle is less (0.55–0.64) compared to CBCT (0.77–0.95)¹⁸. Because the bone tissue must be demineralized sufficiently before becoming noticeable on OPG, which usually takes more than 6 months, the mandibular condyle may appear normal on OPG in the early stages of TMJOA^{19,20}. According to the position paper from the American Academy of Oral and Maxillofacial Radiology (AAOMR), OPG is only useful for diagnosing advanced TMJOA due to its low sensitivity²¹. Image distortion and overlap on OPG are always concerns as well²². However, considering the prominent role of OPG in primary examinations, any supplementary diagnostic tool to screen for TMJOA on OPG would be very helpful in clinics.

The AI algorithm developed in this study showed sufficient sensitivity compared to OMFS experts for the primary diagnosis of TMJOA on OPG. The diagnostic performance (accuracy, 0.51, and F1 score, 0.53) was not satisfying in the initial trial when AI was trained with 3 categories of TMJOA: normal, indeterminate TMJOA, and TMJOA. The Cohen's kappa value for the AI diagnosis on OPG was 0.27, which was less than that of the expert, 0.38, while both represent fair agreement. This implies that it is still difficult to distinguish subtle changes in TMJOA on OPG even for an expert. Besides, multi-label image classification is more challenging than single-label classification²³ as shown in a previous study that reported low performance (mean accuracy, 0.51) for AI classification of lower third molar development into multiple stages for age estimations⁷. Based on this initial result, classification of images was done in different ways.

When indeterminate OA was taken as normal in Trial 1, the AI model performance was best, and showed the highest accuracy, precision, recall, and F1 score (0.80, 0.81, 0.80, and 0.80, respectively). But, Trial 1's sensitivity in diagnostic performance was lowest (0.52). In Trial 2 when indeterminate OA was defined as OA, the model performance (accuracy, 0.73, precision, 0.75, recall, 0.73, and F1 score, 0.74) and specificity (0.23) in diagnostic performance were lowest, while sensitivity was highest (0.97). In Trial 3 when indeterminate OA was omitted from the development process, the model performance (accuracy, 0.78, precision, 0.78, recall, 0.78, and F1 score, 0.78) came close to that in Trial 1, while Trial 3's sensitivity (0.73) and specificity (0.82) were good and more balanced in terms of diagnostic performance. Based on this result, AI performed best for TMJOA diagnosis on OPG when indeterminate OA was omitted during training and verification. The pilot study showed similar accuracy (0.77–0.84) with various AI models when indeterminate OA was omitted¹³.

Indeterminate OA was recategorized as normal in previous studies^{12,14} as in Trial 1 of this study. The sensitivity of the AI (0.52) and expert (0.61) was higher and specificity was lower (0.94 for AI and 0.91 for expert) than those of experts in the previous study (sensitivity, 0.26 and specificity, 0.99)¹⁴. The model performance (accuracy, 0.86 and F1 score, 0.84) in a recent study¹² was better than in Trial 1 of this study (accuracy, 0.80 and F1 score, 0.80) but the materials for AI development were CBCT sagittal images in that previous study. CBCT images have higher detail and fewer artifacts at the anatomical boundaries of the ROIs and background than OPGs²⁴. The superiority of CBCT to OPG in the performance of a DCNN model has already been reported²⁵.

Consequently, the AI algorithm in Trial 3 is the most appropriate for TMJOA diagnosis on OPG, and showed the best balance between sensitivity and specificity among our 3 trials and equivalent diagnostic performance to the expert. Moreover, no statistical difference was observed between the AI diagnosis on OPGs and the expert diagnosis on CBCT only in Trial 3 (McNemar's test, $p = 0.366$), which must be because of a better balance between sensitivity and specificity. This implies that the AI model is more likely to accurately diagnose TMJOA on OPG in accord with expert diagnosis using CBCT when indeterminate TMJOA is excluded from AI training. When the AI in Trial 3 read 115 untested OPG images of indeterminate TMJOA (data not shown), AI was more likely to read indeterminate TMJOA as TMJOA (41 OPGs, 35.7%) than the expert (23 OPGs, 20.0%). Indeterminate TMJOA may be considered a normal variation, aging, physiologic remodeling, or a precursor to TMJOA¹⁵, which means it can be diagnosed as normal and OA at the same time. Because the benefit of high sensitivity may exceed loss of low specificity in the diagnosis of TMJOA where early detection is important, it would be clinically more beneficial for a TMJOA screening tool to read indeterminate OA as OA. In a randomized controlled study, osseous condylar changes in adolescents/young adults with early-stage TMJOA showed repair and even regeneration after conservative and splint therapy²⁶, which may emphasize the need for early detection and management.

Additional statistics were performed to explain Trial 3's model prediction—which included factors correlated with the expert or AI's diagnosis of TMJOA based on the OMFR expert's CBCT reads. Location and types of degenerative bone changes based on CBCT reads by the expert were evaluated by Mann–Whitney test. The expert's diagnosis of TMJOA was correlated with surface erosion ($p = 0.001$) and generalized sclerosis ($p = 0.040$), while AI's diagnosis was correlated with surface irregularity ($p = 0.033$). In this study, AI was trained to learn the whole image with the extracted ROIs, and as a result, it might be said that image overall appearance could influence TMJOA diagnosis rather than specific OA changes. This may explain why AI was closer to CBCT than the expert in diagnosing TMJOA with OPGs.

AI is an up-and-coming method for use in radiology, where a large amount of homogeneous image data are available, and this includes AI's strengths in segmenting, detecting, or classifying organs and lesions. Despite the lack of quality and number of studies, AI has been constantly shown to be equivalent to health-care professionals with respect to diagnostic performance²⁷. On the other hand, AI is more likely to show better results when it is trained with an ROI image than with a whole image²⁸. However, ROIs are extracted manually in most studies, which can compromise AI's practical usability. In this study, an AI algorithm was designed to extract ROIs from OPG images based on an object detection technique. The average precision of mandibular condyle detection was reported to be 99.4% on right side and 100% on left side in a previous study¹³. The ROI extracted automatically for this study covered the mandibular condyle, and the articular fossa and eminence, which is very important because TMJOA is not defined only by bony changes in the condyle. It is obvious that OA changes occur in other structures of the TMJ such as the fossa and eminence²⁹, so that the ROI for AI diagnosis should cover all structures of the joint, rather than just the condyle. But, most TMJOA studies usually focus on the condyle and only one AI study based on TMJ CBCT also used the mandibular condyle as extracted from sagittal sections¹².

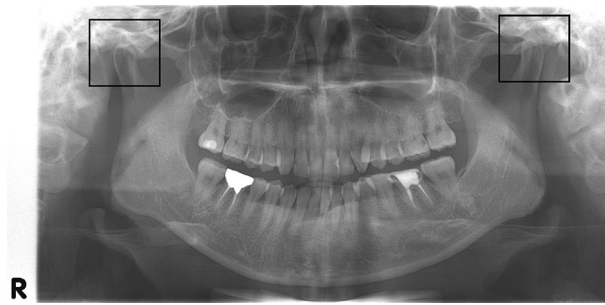


Figure 2. Result of ROI extraction, 300×300 pixels.

This study has several limitations. First, the absolute size of the training dataset was rather small. The use of a larger dataset for training and/or external validation may render different findings. In order to overcome the limitation of a small size dataset, data augmentation by image modification and a transfer learning technique with fine-tuning based on an imagenet database (<http://image-net.org>) were used. It has been reported that the accuracy of transfer learning increases to some extent for medical images rather than general objects³⁰. Although AI did not exceed an expert with respect to accuracy in this study, this may improve in further studies with larger datasets, learning OPG and CBCT images together, elaborating deep learning models using landmarks, and an ensemble composed of multiple AI models. Second, it is well known that an external test dataset drawn from multiple medical centers secures high AI performance for reproducibility in general use. However, this study was based on an internal dataset, but, recently, there is no noticeable difference in performance between OPG devices from various manufacturers. Last, deep learning algorithms have inherent uncertainty³¹. Compared to machine learning methods based on handcrafted features, the trained deep learning model is like a “black-box” so the results are not explainable³².

Conclusions

Collectively, an AI may read OPGs to diagnose TMJOA as well as OMFR experts can with respect to sensitivity and has greater accordance with CBCT interpretations than do OMFR experts, which implies that AI can play an important role in diagnosing TMJOA primarily from OPGs in most general practice clinics, where OMFR experts or CBCT are not available.

Methods

Materials. The written documentation of informed consent was waived and approved by the decision of the Institutional Review Board of School of Dentistry, Seoul National University (S-D20200004) and ethics committee approval for the study in the same institute was also obtained. All methods were performed in accordance with relevant guidelines and regulations. Radiographic images of the patients who visited the orofacial pain clinic of Seoul National University Dental Hospital who reported TMD-related symptoms and had an OPG (Orthopantomograph OP, 100D, Instrumentarium Corporation, Tuusula, Finland) and TMJ CBCT (SOMATOM Sensation 10, Siemens, Erlangen, Germany) which were read by OMFR specialists from January, 2015 to October, 2019 were reviewed. Records of patients under 18 years of age or with a history of orthognathic surgery, macro trauma, and systemic diseases that could cause joint deformity or with a temporal difference of more than 3 months between OPG and CBCT imaging were excluded. The AI algorithm was trained, validated, and tested with 1189 OPGs, all of which had been confirmed by additional CBCT examination, selected randomly and classified by an orofacial pain specialist in terms of image analysis criteria for the diagnosis of temporomandibular disorder (research diagnostic criteria for TMD¹⁴; diagnostic criteria for TMD¹⁵: no TMJOA (normal), indeterminate for TMJOA (indeterminate), and TMJOA (OA). Among 2378 joints, 800 were diagnosed as normal, 779 as indeterminate, and 799 as OA based on the CBCT reads (Table 1).

AI model development. First, an algorithm to extract regions of interest (ROI) including the mandibular condyle and surrounding structures from each OPG by object detection was developed (Fig. 2). The objective detection technique was based on Faster Regions with Convolutional Neural Networks (RCNN) using the Inception V3 model as the categorizing algorithm in which Region Proposal Network (RPN) and Image Classification Network (ICN) work simultaneously and make it faster. The RCNN used an algorithm called selective search to extract approximately 2000 areas where there were likely objects. This technique is called region proposals. For each region, 4096-dimensional feature vectors were derived using CNN for image classification (Inception ResNet V2 was used in this paper). The CNN model took a 227×227 color image as the input and derived the included characteristics through 5 convolutional layers and 2 fully-connected layers. Therefore, region proposals must be warped to a size of 227×227 before putting them into the CNN. Then, a support vector machine was used to predict the class associated with the feature vector. Finally, Bounding-box (BB) regression was performed to determine the location of the objects more accurately. In the next step, extracted ROI images were classified as normal, indeterminate, and OA by means of the Keras' ResNet model based on a Convolutional Neural Network (CNN). The ROI images of 2378 joints were divided randomly into training (1478 images), validation (450 images), and test sets (450 images), with which the AI algorithm was developed using Keras' ResNet

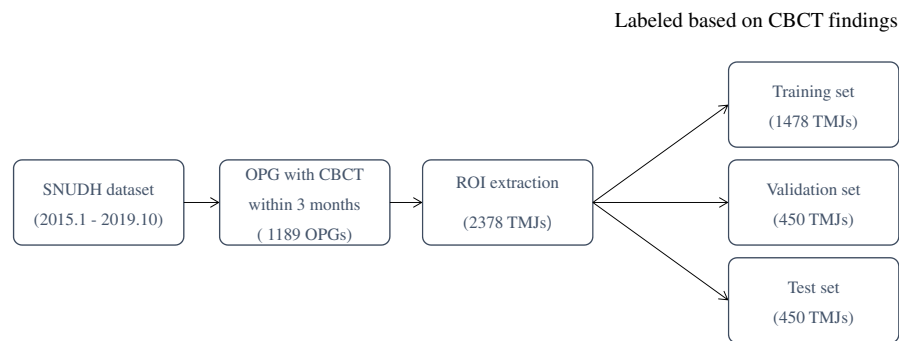


Figure 3. Clinical datasets used for training, validation, and test.

model. The test set consisted of 150 normal, 150 indeterminate, and 150 OA images (Fig. 3). Data augmentation was done by image rotation ± 5 degrees, image shift $\pm 10\%$, brightness $\pm 10\%$, and contrast $\pm 10\%$ to compensate for the disadvantage of the small number of the data points to increase model robustness. Training and validation were repeated 35,000 times (700 epochs) with augmented data. The learning rate of the model was 1.0×10^{-6} and an Adam optimizer was used. After 700 training epochs, the validation loss of the model decreased from 12.2 to 0.1. In order to find the most suitable model for screening TMJOA, Indeterminate OA was treated as follows during AI model development.

1. Initial trial: Indeterminate OA was treated independently.
2. Trial 1: Indeterminate OA was considered normal.
3. Trial 2: Indeterminate OA was considered TMJOA.
4. Trial 3: Indeterminate OA was omitted.

After selecting the optimal trial, five-fold cross validation was performed to evaluate model training, while avoiding overfitting or bias. The 1599 images consisting of 800 normal and 799 OA selected as the training dataset were randomly divided into five folds. Within each fold, the dataset was partitioned into independent training and validation sets, using an 80 to 20 percentage split. The selected validation set was a completely independent fold from the other training folds, and it was used to evaluate model training status during the training. After one model training step was completed, the other independent fold was used as a validation set and the previous validation set was reused, as part of the training set, to evaluate the model training.

Model and statistical analysis. Accuracy, precision, recall, and F1 score were calculated for model performance. Accuracy is defined as the ratio of correct predictions. Precision is the ratio of true positives to true positives and false positives. Recall is the ratio of true positives to true positives and false negatives. Finally, the F1 score is a harmonic mean of precision and recall: $(2 \times \text{precision} \times \text{recall}) / (\text{precision} + \text{recall})$. Accuracy, specificity, and sensitivity were calculated for diagnostic performance, Cohen's kappa was calculated to estimate the agreement of TMJOA diagnosis between OPG and CBCT reads, and McNemar's test was done to evaluate the significance of difference. For evaluation of AI clinical usability, the results between OPG reads by the AI and the expert were compared. All p values < 0.05 were considered to be statistically significant. The Python programming language (v. 3.6), Tensorflow (v. 2.0) and a graphics card (GeForce GTX 2080) were used for analysis.

Data availability

The data that support the findings of this study are available from the authors upon reasonable request.

Received: 21 December 2020; Accepted: 27 April 2021

Published online: 13 May 2021

References

1. Wang, X., Zhang, J., Gan, Y. & Zhou, Y. Current understanding of pathogenesis and treatment of TMJ osteoarthritis. *J. Dent. Res.* **94**, 666–673 (2015).
2. Buckwalter, J. A., Mankin, H. J. & Grodzinsky, A. Articular cartilage: Degeneration and osteoarthritis. *Instr. Course Lect.* **54**, 465 (2005).
3. Schiffman, E. L. *et al.* The research diagnostic criteria for temporomandibular disorders. I: overview and methodology for assessment of validity. *J. Oral Facial Pain Headache* **24**, 7 (2010).
4. Larheim, T., Abrahamsson, A., Kristensen, M. & Arvidsson, L. Temporomandibular joint diagnostics using CBCT. *Dentomaxillofac. Radiol.* **44**, 20140235 (2015).
5. White, S. C. & Pharoah, M. J. *Oral Radiology: Principles and Interpretation (4th edition)* 493–498 (Mosby, 2009).
6. Wirtz, A., Mirashi, S. G. & Wesarg, S. Automatic teeth segmentation in panoramic X-ray images using a coupled shape model in combination with a neural network. *Med. Image Comput. Comput. Assist. Interv.* **11073**, 712–719 (2018).
7. De Tobel, J., Radesh, P., Vandermeulen, D. & Thevissen, P. W. An automated technique to stage lower third molar development on panoramic radiographs for age estimation: A pilot study. *J. Forens. Odontostomatol.* **35**, 42 (2017).

8. Vinayahalingam, S., Xi, T., Bergé, S., Maal, T. & de Jong, G. Automated detection of third molars and mandibular nerve by deep learning. *Sci. Rep.* **9**, 1–7 (2019).
9. Yang, H. *et al.* Deep learning for automated detection of cyst and tumors of the jaw in panoramic radiographs. *J. Clin. Med.* **9**, 1839 (2020).
10. Lee, K.-S., Jung, S.-K., Ryu, J.-J., Shin, S.-W. & Choi, J. Evaluation of transfer learning with deep convolutional neural networks for screening osteoporosis in dental panoramic radiographs. *J. Clin. Med.* **9**, 392 (2020).
11. Murata, M. *et al.* Deep-learning classification using convolutional neural network for evaluation of maxillary sinusitis on panoramic radiography. *Oral Radiol.* **35**, 301–307 (2019).
12. Lee, K. *et al.* Automated detection of TMJ osteoarthritis based on artificial intelligence. *J. Dent. Res.* **99**, 1363–1367 (2020).
13. Kim, D., Choi, E., Jeong, H. G., Chang, J. & Youm, S. J. Expert system for mandibular condylar detection and osteoarthritis classification in panoramic imaging using R-CNN and CNN. *Appl. Sci.* **10**, 7464 (2020).
14. Ahmad, M. *et al.* Research diagnostic criteria for temporomandibular disorders (RDC/TMD): Development of image analysis criteria and examiner reliability for image analysis. *Oral Surg. Oral Med. Oral Pathol. Oral Radiol. Endod.* **107**, 844–860 (2009).
15. Schiffman, E. *et al.* Diagnostic criteria for temporomandibular disorders (DC/TMD) for clinical and research applications: Recommendations of the International RDC/TMD consortium network and orofacial pain special interest group. *J. Oral Facial Pain Headache* **28**, 6 (2014).
16. Kim, K., Wojczyńska, A. & Lee, J.-Y. The incidence of osteoarthritic change on computed tomography of Korean temporomandibular disorder patients diagnosed by RDC/TMD; a retrospective study. *Acta Odontol. Scand.* **74**, 337–342 (2016).
17. Jeon, Y.-M. *et al.* The validity of computed tomography in diagnosis of temporomandibular joint osteoarthritis. *J. Oral Med.* **33**, 195–204 (2008).
18. Honey, O. B. *et al.* Accuracy of cone-beam computed tomography imaging of the temporomandibular joint: Comparisons with panoramic radiology and linear tomography. *Am. J. Orthod. Dentofacial Orthop.* **132**, 429–438 (2007).
19. Kamelchuk, L. S. & Major, P. W. Degenerative disease of the temporomandibular joint. *J. Orofac. Pain* **9**, 168–180 (1995).
20. Cibere, J. Do we need radiographs to diagnose osteoarthritis?. *Best Pract. Res. Clin. Rheumatol.* **20**, 27–38 (2006).
21. Brooks, S. L. *et al.* Imaging of the temporomandibular joint: A position paper of the American Academy of Oral and Maxillofacial Radiology. *Oral Surg. Oral Med. Oral Pathol. Oral Radiol. Endod.* **83**, 609–618 (1997).
22. Mawani, F. *et al.* Condylar shape analysis using panoramic radiography units and conventional tomography. *Oral Surg. Oral Med. Oral Pathol. Oral Radiol.* **99**, 341–348 (2005).
23. Deng, J. *et al.* Imagenet: A large-scale hierarchical image database. in *2009 IEEE Conference on Computer Vision and Pattern Recognition*. 248–255 (2009).
24. Scarfe, W. C., Farman, A. G. & Sukovic, P. Clinical applications of cone-beam computed tomography in dental practice. *J. Can. Dent. Assoc.* **72**, 75 (2006).
25. Lee, J. H., Kim, D. H. & Jeong, S. N. Diagnosis of cystic lesions using panoramic and cone beam computed tomographic images based on deep learning neural network. *Oral Dis.* **26**, 152–158 (2020).
26. Lei, J., Yap, A. U. J., Liu, M. Q. & Fu, K. Y. Condylar repair and regeneration in adolescents/young adults with early-stage degenerative temporomandibular joint disease: A randomised controlled study. *J. Oral Rehab.* **46**, 704–714 (2019).
27. Liu, X. *et al.* A comparison of deep learning performance against health-care professionals in detecting diseases from medical imaging: A systematic review and meta-analysis. *Lancet Dig. Health* **1**, e271–e297 (2019).
28. Do, S., Song, K. D. & Chung, J. W. Basics of deep learning: A radiologist's guide to understanding published radiology articles on deep learning. *Korean J. Radiol.* **21**, 33–41 (2020).
29. O'Ryan, F. & Epker, B. N. Temporomandibular joint function and morphology: Observations on the spectra of normalcy. *Oral Surg. Oral Med. Oral Pathol.* **58**, 272–279 (1984).
30. Poedjiastoeti, W. & Suebnukarn, S. Application of convolutional neural network in the diagnosis of jaw tumors. *Health Inform. Res.* **24**, 236–241 (2018).
31. Gal, Y. Uncertainty in deep learning. in *Los Altos: IEEE/ACM Transactions on Audio, Speech, and Language Processing* (2017).
32. Holzinger, A. From machine learning to explainable AI. in *2018 World Symposium on Digital Intelligence for Systems and Machines (DISA)*. Piscataway: IEEE. 55–66 (2018).

Author contributions

E.C. and H.-K.P. contributed to conception, design, and acquisition of data. E.C. and D.K. analyzed data. E.C., J.-Y.L. and H.-K.P. wrote the manuscript text and prepared figures and tables. All authors reviewed the manuscript.

Competing interests

The authors declare no competing interests.

Additional information

Correspondence and requests for materials should be addressed to H.-K.P.

Reprints and permissions information is available at www.nature.com/reprints.

Publisher's note Springer Nature remains neutral with regard to jurisdictional claims in published maps and institutional affiliations.



Open Access This article is licensed under a Creative Commons Attribution 4.0 International License, which permits use, sharing, adaptation, distribution and reproduction in any medium or format, as long as you give appropriate credit to the original author(s) and the source, provide a link to the Creative Commons licence, and indicate if changes were made. The images or other third party material in this article are included in the article's Creative Commons licence, unless indicated otherwise in a credit line to the material. If material is not included in the article's Creative Commons licence and your intended use is not permitted by statutory regulation or exceeds the permitted use, you will need to obtain permission directly from the copyright holder. To view a copy of this licence, visit <http://creativecommons.org/licenses/by/4.0/>.

© The Author(s) 2021